Office translation

Material Testing Laboratory
of the State of Brandenburg -
Instructed to perform material
testing for the state Berlin

Examination Report

No. 1.3/00/3664

2 copies

Client	TOP STORY Filmproduktion GmbH Mrs. Jutta Rabe August-Bebel-Straße 26-53 14482 Potsdam
Contents	Material examination of a part of the starboard front bulkhead of the ferry "Estonia" in order to prove mechanically caused structure deformations.

Instructions received	06.09.2000
Material received	01.09.2000
Material delivered by	client
Time period of examination	08.09.2000 to 28.09.2000

1. Contents of Instructions

The part supplied from the starboard front bulkhead of the ferry "Estonia" was according to agreement examined as follows:

- Scanning electron microscope (SEM) examination
- Chemical composition (piece analysis)
- Metallographic examinations
- Micro hardness process measurements
- Examination report

2. Statements Concerning the Objects to be Examined

2.1 Object to be examined

The triangular steel sample of the starboard front bulkhead has according to clients two sides (cathedes) which are fracture edges and one side (hypotenuse) which was flame-cut during cutting off of the sample. The fracture edges and the parts of the surfaces are corroded. The area marked side 1 shows besides red paint remains also partly broken parts of the white top layer. This side is according to clients the outside of the bulkhead. The area marked side 2 is, besides the mentioned corroded parts, exclusively covered by white paint. (Pictures 1, 2.)

2.2 Preparations of Specimen

After the drawing up of a sample plan (picture 7) macroscopic overview photos were made (pictures 1 – 6) and the material separated for the different examinations.

The SEM examinations were carried out at the non-treated fracture areas and thereafter at one specimen after removal of the loose corrosion products.

In order to determine the chemical composition a facing and a polish specimen were made of the respective sample.

The metallographic specimens were micro-cut, imbedded, treated and structured.

Table 1: Distribution of specimen and markings.

Run. No.	Specimen Mark of Client	Mark of Specimen	Type of Specimen	Remarks
1	PART OF STARBOARD FRONT BULKHEAD	13/00/3664 V011	fracture surface	SEM examination
2		13/00/3664 V021	fracture surface	SEM examination
3		13/00/3664 S011	facing section	piece analysis
4		13/00/3664 G011	section, middle micro instead of cross	structure, area distant from the fracture edge
5		13/00/3664 G012	section from the middle opposite G011 turned by 90°	structure, area distant from the fracture edge
6		13/00/3664 HMV012	at section G012	Micro-hardening process

7		13/00/3664 G021	section parallel to fracture edge	structure, pages ¾ fracture edge
8		13/00/3664 G022	section transverse to fracture edge	structure, pages ¾ fracture edge
9		13/00/3664 HMV022	section G022	Micro-hardening process
10		13/00/3664 G031	section parallel to fracture edge	structure, pages ¾ fracture edge
11		13/00/3664 G032	section transverse to fracture edge	structure page 3, fracture edge
12		13/00/3664 HMV032	at section G032	Micro-hardening process

3. Examination carried out and Results

3.1 SEM Examinations

Examination technique : Topographic and analytic examinations of fracture surfaces

Examination installation : SEM digital scanning microscope DSM 940 A of Messrs. CARL ZEISS OBERKOCHEN with EDX set of Messrs. LINK/OXFORD INSTRUMENTS LTD.

Examination results:

Due to the extensive corrosion appearance it was no more possible to establish on the fracture surface indications of its characteristics. The fracture surface does not show a uniform appearance picture. Besides the areas with a thick layer of corrosion products - specimen 1.3/00/3664 V021 (picture 8) and specimen 1.3/00/3664 V011 (picture 10) – there are areas recognizable where part of the corrosion layer is cracked off (pictures 11 and 12). The chemical composition of the surface areas shown by the pictures is compiled in *Table 2*. The composition of the fracture surface area with the thick corrosion layer shows a high iron and oxygen content as well as a relatively high silicium concentration, which cannot be explained by the silicium content of the steel (*Table 2, column 2-4)*. The silicium distribution of the fracture surface area shown on picture 8 is shown on picture 9. Accordingly the silicium is mainly present in 5-10 µm big particles. It has to be assumed that small sand particles are contained in the layer of corrosion products.

Besides the mentioned elements also sulphur is contained in considerable quantities in this layer. The other elements mentioned in *Table 2* can in substance be traced back to sea water, whereby it has to be noted that chlorine was not found in these fracture surface areas.

In the fracture surface areas, where a part of the layer of corrosion products was cracked off (pictures 11 and 12) also a sulphur concentration of more than 10% – besides a high content of oxygen and iron – could be determined *(Table 2, columns 5, 6)*. It is not possible to determine by means of the results of the analysis in which chemical bound form the sulphur is present. The source for the sulphur contamination cannot be stated. Based on the analysis of the attached paint remains the coating can be excluded as the source of the sulphur supply.

Table 2 : Compilation (element %) of the different fracture surface areas (element %).

	1.3/00/3664 VO21	1.3/00/3664 VO11	1.3/00/3664 VO21	1.3/00/3664 VO21	1.3/00/3664 VO11
Element	Picture 8	Picture 10	Picture 11 Position 1	Picture 11 Position 2	Picture 12
1	2	3	4	5	6
OXYGEN (O)	45,2	34,7	43,4	24,5	29,7
SODIUM (Na)	0,7	0,8	1,5	0,0	0,9
MAGNESIUM (Mg)	0,2	0,6	0,5	0,8	0,4
ALUMINIUM (Al)	0,4	0,1	0,2	0,0	0,0
SILICIUM (SI)	1,8	1,5	2,3	0,1	3,1
PHOSPHORUS (P)	0,4	0,6	0,7	0,0	0,2
SULPHUR (S)	1,0	1,5	1,2	11,6	14,5
POTASSIUM (K)	0,1	-	0,1	0,0	0,0
CALCIUM (Ca)	0,1	0,3	0,2	0,2	0,1
CHROMIUM (Cr)	0,0	0,0	0,0	0,0	0,0
MANGANESE (Mn)	0,0	0,0	0,0	0,0	0,0
IRON (Fe)	50,0	59,9	49,8	62,8	51,1

Picture 13 shows a fracture surface area with the layer of corrosion products having been more or less cracked-off (specimen 1.3/00/3664 V011). The chemical composition of this fracture surface area is stated in *Table 3, column*

2. In the fracture surface area only to a small extent covered by corrosion products small quantities of nickel are present. Nickel as well as chrome and manganese could also be proved in those parts of the fracture surface *(Table 3, column 3)* where the thick layer of corrosion products had been removed mechanically (picture 14). While the manganese being an alloy part is present in non-alloyed building steels, the contents of nickel and chrome cannot be explained. On the SEM picture of this fracture surface area (picture 14) a crack is visible. It cannot be excluded that in addition to this fracture (through-running crack) further cracks (secondary cracks) do exist in the material.

Table 3 : Composition (element %) of different fracture surfaces and surface areas.

	1.3/00/3664 VO11	1.3/00/3664 VO11	1.3/00/3664 VO21	1.3/00/3664 VO21	1.3/00/3664 VO21
Element	Picture 13	Picture 14	Picture 15	Picture 16	Picture 17
1	2	3	4	5	6
OXYGEN (O)	5,9	33,6	31,2	23,5	12,4
SODIUM (Na)	0,1	0,9	0,7	0,0	0,4
MAGNESIUM (Mg)	0,1	0,0	0,0	1,4	0,6
ALUMINIUM (Al)	0,0	0,0	0,5	0,0	0,0
SILICIUM (Si)	0,1	0,3	2,2	0,1	1,1
PHOSPHORUS (P)	0,0	0,0	0,6	0,0	0,1
SULPHUR (S)	0,8	4,3	1,0	12,5	0,6
CHLORINE (Cl)	0,0	0,2	0,1	0,0	0,0
POTASSIUM (K)	-	0,0	0,3	0,0	0,0
CALCIUM (Ca)	0,0	0,0	0,1	0,3	0,2
TITANIUM (Ti)	0,0	0,0	-	0,0	0,1
CHROMIUM (Cr)	0,0	0,1	0,0	0,0	0,2
MANGANESE (Mn)	0,0	0,3	0,0	0,0	0,7
IRON (Fe)	92,8	59,7	63,2	62,1	81,2
NICKEL (Ni)	0,2	0,6	0,0	0,0	1,3
COPPER (Cu)	0,0	0,0	0,0	0,0	0,9

For the purpose of comparison areas of the inner surface near the fracture edge have been examined. Pictures 15-17 (specimen 1.3/00/3664 V021) show respective surface areas and their chemical composition is shown in columns 4

to 6 of *Table 3*. The appearance forms of the corroded areas of the inner surface are similar to those of the fracture surface. The surface area with completely attached corrosion layer consists mainly of the oxidizing products of iron *(Table 3, column 4)*. Similar to the composition of the fracture surface *(Table 2, columns 2-4)* also at the inner surface increased concentrations of silicium and sulphur are present. Also at the areas of the inner surface, where the layer of corrosion products is partly cracked off, the composition of the respective areas complies with the fracture surface, i.e. also in areas of the inner surface a sulphur content of more than 10% has been established. In way of the area of the inner surface (picture 17) where the layer of corrosion products was mostly cracked off, the elements nickel (1.3%), copper (0.9%) and chromium (0.2%) could be proved. These elements are neither parts of the steel nor of the coating.

3.2 Chemical Composition (piece analysis)

Specimen treatment	Facing and polish micro-sections
Testing installation	glow discharge spectral-meter

Testing result

The analysis result is shown in *Table 4, page 31*. The chemical composition of the specimen determined can be compared with building steel St 37-2, material no. 1.0037 according to EN 10025 (*Table 4*).

The specimen 1.3/00/3664 S011 shows within the tolerances a particularly low sulphur content.

3.3 Structure examination

3.3.1 Metallographic examination

Examination technique	:	Metallographic treatment, etching technique and light microscopy
Examination installation	:	Automatic polishing set TF 250 JEAN WIRTZ, stereo-microscope CZ JENA GMBH, Camera uplight microscope Neophat 32 CZ JENA GMBH, Picture analysis system Imtron 2000 Messrs. IMTRONIK GMBH

Examination results

The micro sections of the specimens 13/00/3664 G011 and 13/00/3664 G012 were taken from the presumably less strained area of the fracture occurrence.
The take-away location is ca. 5 cm off the fracture edges and ca. 3 cm off the flame-cut hypotenuse.
The specimen 13/00/3664 G031, extending into the flame-cut area, revealed a welding strain through the different heat diffusion zones up to a distance of max. 6 mm. Consequently it has to be concluded that specimens 13/00/3664 G011 and 13/00/3664 G012 did not sustain structure changes due to heat as a result of the flame-cutting process.
The metallographic examinations of specimen 13/0073664 G011 and 13/00/3664 G012 revealed a fine, recrystallized, slightly lalmellar ferrite, perlite structure with manganese sulphide slag and secondary cementite precipitations along the grain edges. The structure mainly consists of ferrite.
The perlite is structured fine to middle lamellar and built up distinctly lamellar. The light microscope examination did not reveal any changes by eventual mechanical influences (pictures 18-21). This structural condition can be compared with the structure of a finely granular non-alloyed building steel.
The micro sections of specimen 13/00/3664 G021 and 13/00/3664 G022 as well as 13/00/3664 G031 and 13/00/3664 G032 have been taken from the fracture areas of the steel sample (sample plan, picture 7).
There are significant differences of the structure conditions in the micro sections of the specimens recognizable which depend on the place from where the specimens were taken.

The structure of specimen 13/00/3664 G021, which had been taken ca. 1 cm off the fracture edge (turned 90° as to specimen 13/00/3664 G022), shows only minor changes (picture 22, 23), as for example slight changes in the perlite grain (picture 23), which is partly still granular and partly a destruction of the lamellae in the grain is visible. The grain is compared to the grain of specimens 13/00/3664 G011 and 13/00/3664 G012 slightly stretched (picture 22).

The structure of specimen 13/00/3664 G022 shows significant changes in way of the fracture edge area (pictures 26-33). These plastic deformations in the micro range do indicate exposure to extremely heavy shock forces such as happens from the effects of a substance detonating.

The resulting heat, which is created during such a shock by the internal friction whilst overcoming the sliding resistance, is responsible for the changes within the structure. Since the sliding does not occur in phases but undulatively (as a consequence of the movements of displacements), this is also recognizable as undulative formation of the structural parts (pictures 26-33). The shearing bands created are in particular clearly visible on the pictures 27 and 28. The initial structural parts are extensively destroyed. On the overview of the micro section of specimen 13/00/3664 G022, pictures 24 and 25, the undulative condition of the structural parts is recognizable also in the macro range. The undulative condition of the fracture edge is located at the inside of the bulkhead.

Whether the jagged lines on the right hand side of picture 32 indicate internal cracks has to be established by further examinations.

The in volume panel-shaped iron carbide parts of the perlite are unable to resist the strong micro processes. The destruction of this perlite, marked on the micro section as lamellar structure, becomes particularly clear on pictures 29, 31 and 33. A destruction of the lamellae has occurred which cannot occur by any comparable mechanical technological influence. The processes of explosive treatments of metallic materials as for example explosive hardening and explosive cladding have to be excluded. These processes show in surface-near areas comparable effects.

The structures of specimen 13/00/3664 G031 (pictures 34-37) also show only minor changes, comparable to those of specimen 13/00/3664 G021, which is primarily recognizable by a change of the perlite grain (picture 35).
Also here it is established that there are slight changes in the perlite grain (pictures 35, 37), which partly is still lamellar and which partly shows a destruction of the lamellae in the grain. Stretching of the grains in comparison to the grains of the specimen 13/00/3664 G011 and 13/00/3664 G012 is hardly visible (picture 22).

3.3.2 Measurements of the micro hardening development

Examination technique : Metallographic treatment, micro hardening measurement

Examination installation : Micro hardening examination set, computer controlled HMV2000, SHIMADZU

Examination results

The hardening development measurements have been performed from the edge (fracture edge respectively surface side 1) to the core of specimen 13/00/3664 G012, 13/00/3664 G022 and 13/00/3664 G032 (perpendicular to the fracture edge).
For a better recording of the hardening in the edge-near area the micro hardening development measurements were performed by HV 0.05 (small indentation diagonal). In the immediate vicinity of the surfaces the respective measuring point 1 is situated.
The results of the measurements are listed up in tables 5, 6 and 7 (pages 32-34).
The hardening values of steel ST37-2 used for comparison purposes have been established to be in the range between HV 105 to HV 145 after change of the tensile strength Rm to Vickers HV. The lowest hardening values measured of the specimen are with HV 281 substantially higher than the hardening values of an uninfluenced material of this class.
It has to be concluded that the pressure waves also in areas, where by means of light microscopes, only little deformation is recognisable, did result in

hardening due to structure deformation in the micro range; (deformation of the perlite grain, change of the solidification density).
In way of measuring point 1 of specimen 13/00/3664 G022 the strongest hardening was measured to be HV 515. The hardening values of fracture distant specimen 13/00/3664 G012 show the same increase of hardening as the other specimen, however, without reaching the peak values in the fracture near areas.
The fluctuations of the hardening values do result from the small force (small indentation diagonals) on the recording of small structure areas, which are different in their hardening (soft ferrite, hard perlite).

4. Summary and Discussion of Results

In order to prove mechanically caused changes of the grain structure material testings were performed. Due to the strong corrosion appearances on the fracture surface the fracture characteristics could no more be established by means of scanning electron microscopic examination. The composition of the surface areas by a thick corrosion layer shows a high content of iron and oxygen and a distinct silicium concentration, which cannot be explained by the silicium content of the steel. In way of the fracture areas with partly cracked off corrosion layer sulphur concentrations of more than 10 p.c. could be proved in addition to oxygen and iron contents. The source of the sulphur contamination cannot be stated.
In way of the surface areas, where the cracking off of the corrosion layer was far-reaching, small quantities of nickel have been analysed. Nickel as well as chrome and manganese could also be proved in way of the areas where the thick corrosion layer had been removed mechanically. The contents of the nickel and chrome cannot be explained.
In way of an area of the inner surface with far-reaching cracked off corrosion layer – apart from nickel (1.3%) and chrome (0.2%) – also copper (0.9%) could be proved.
The chemical composition of the sample was established and compared with building steel St 37-2, material no. 1.00037, according to EN 10025. The

analysed sample has within the tolerances a particularly low phosphorus content.

The metallographic examinations of the micro sections from the less strained area revealed a fine, recrystallized, slightly lamellar ferrite, perlite structure with manganese sulphide slag and secondary cementite precipitations along the grain edges. The major proportion of the structure is ferrite. The perlite is structured fine to middle lamellar and clearly built up lamellated. This structure picture is comparable to the structure of a fine-grained, unalloyed building steel.

The strained micro-section specimens from the fracture area of the starboard front bulkhead show an extensive destruction of the initial structure components. These plastic deformations within the micro range indicate exposure to extremely heavy shock forces, such as happens from the effects of a substance detonating.

The resulting heat, which is created during such a shock by the internal friction whilst overcoming the sliding resistance, is responsible for the changes within the structure. Since the sliding does not occur in phases but undulatively (as a consequence of the movements of displacements) this is also recognizable as undulative formation of the structural parts. Already at a distance of ca. 9 cm from the specimen strained strongest only little changes to the structural characteristics were established.

Based on these results it is probable that the main strained area is to be found at another part of created hole.

During the micro hardness process measurements the hardness values have been compared with those of the St 37-2 steel. According to the established revaluation of tensile strength Rm of St 37-2 steel the hardness values should have been within a range of HV 105 to HV 145. The lowest hardness value of the measured specimen is with HV 281, however substantially higher than the hardness values of an uninfluenced material of this class.

It has to be concluded that the pressure waves also in areas, where by means of light microscopes, only little deformation is recognisable, did result in

hardening due to structure deformation in the micro range; (deformation of the perlite grain, change of the solidification density).
The highest hardening has been established in way of the immediate fracture area of the specimen being most strongly strained.
For this hardness increase as well as for the determined structure deformations detonative influence is probable.

Berlin, 29.9.00

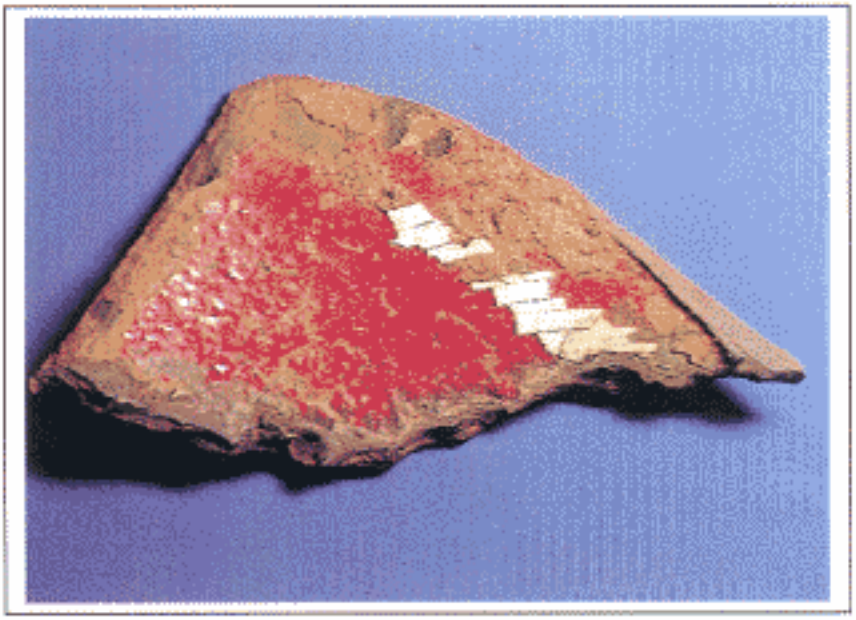

Bild 1 Probe 1.3/00/3664
Seite 1

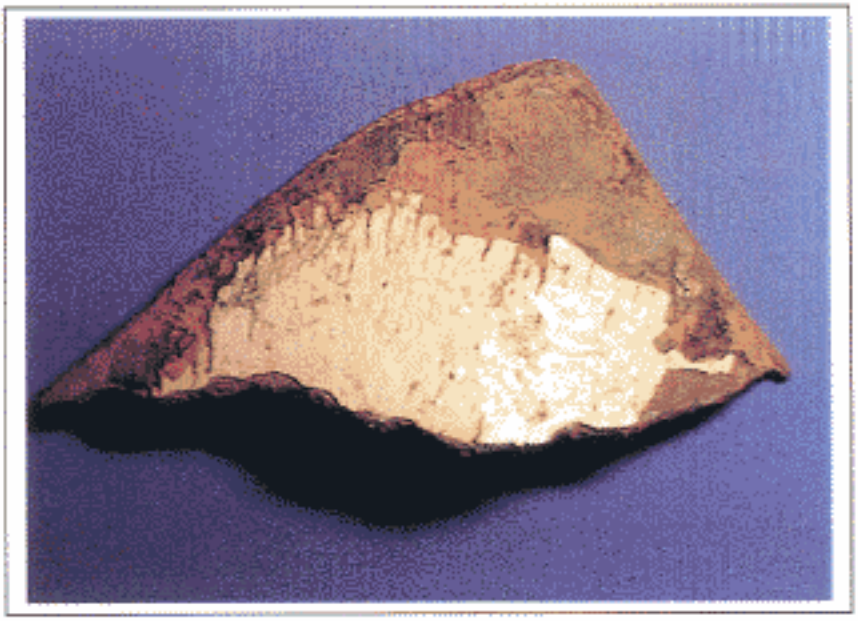

Bild 2 Probe 1.3/00/3664
Seite 2

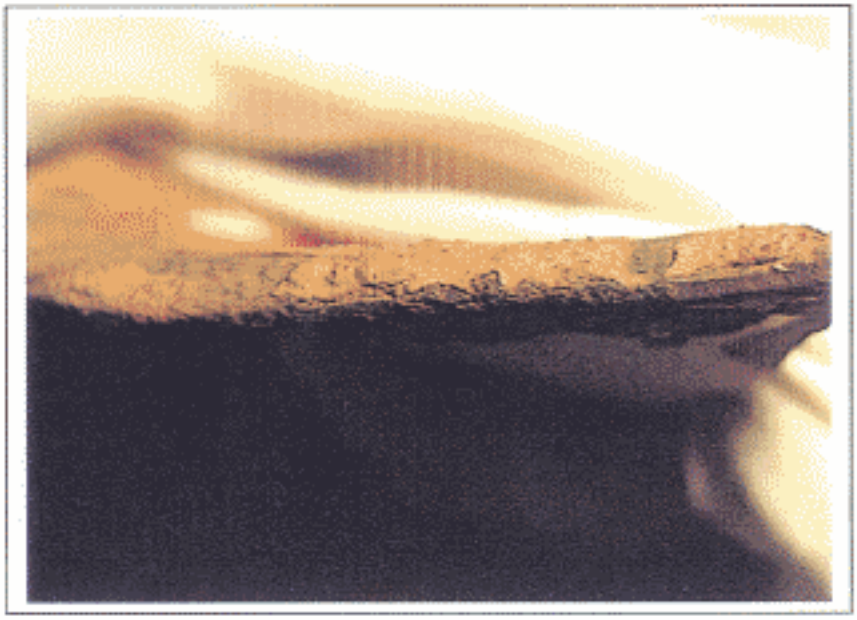

Bild 3 Probe 1.3/00/3664
Seite 3

Bild 4 Probe 1.3/00/3664
Seite 4

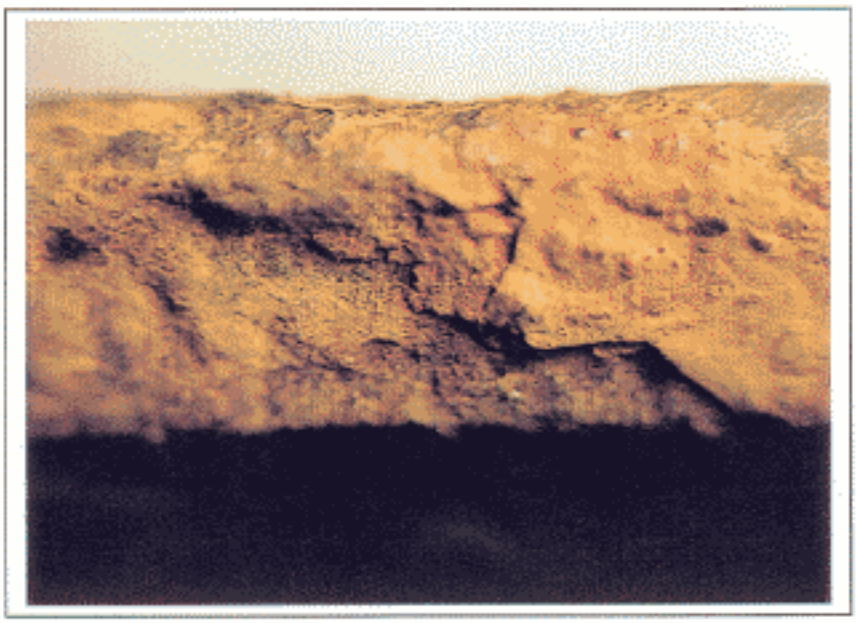

Bild 5 Probe 1.3/00/3664
Seite 3, Ausschnitt

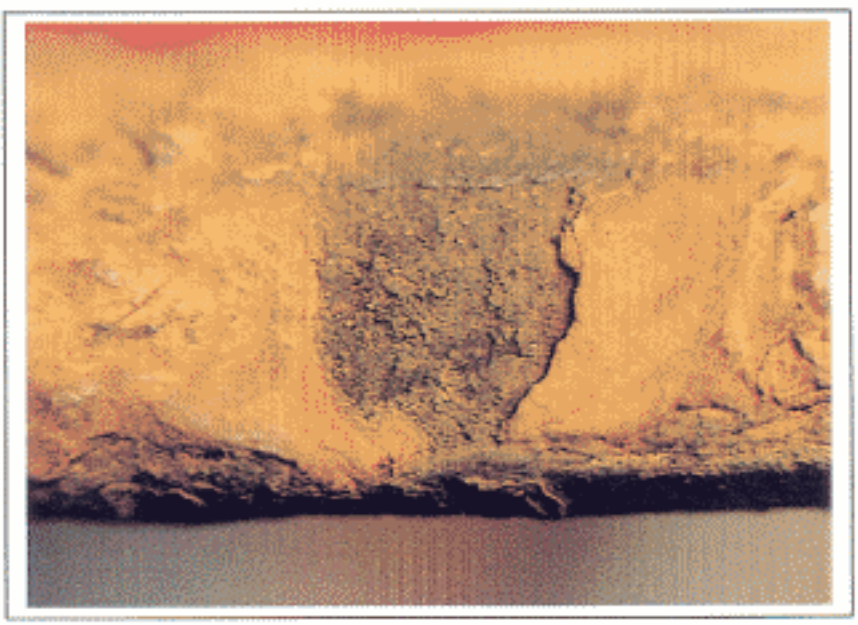

Bild 6 Probe 1.3/00/3664
Seite 4, Ausschnitt

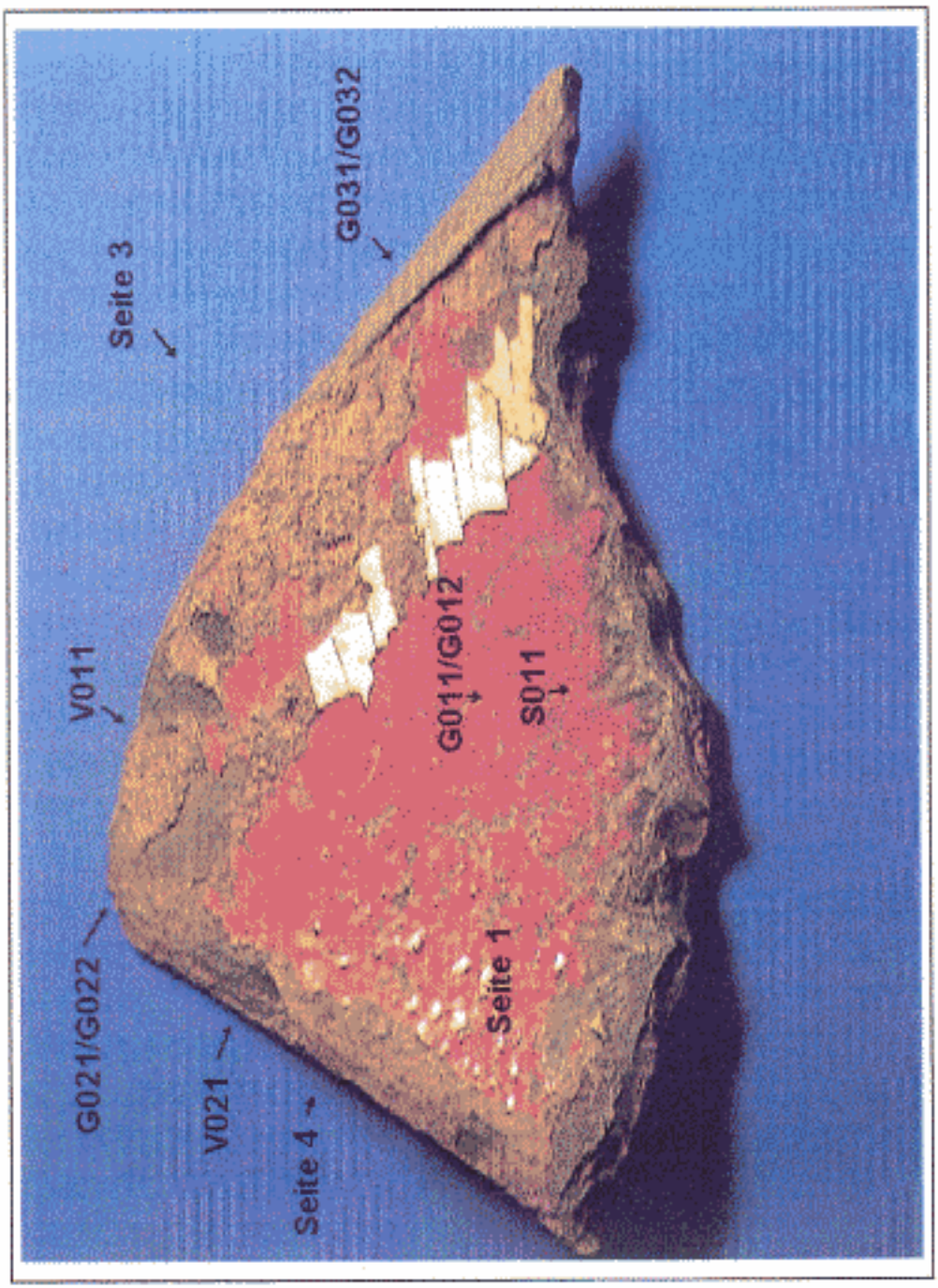

Bild 7 Probe 1.3/00/3664, Probenplan ca.: 1:1

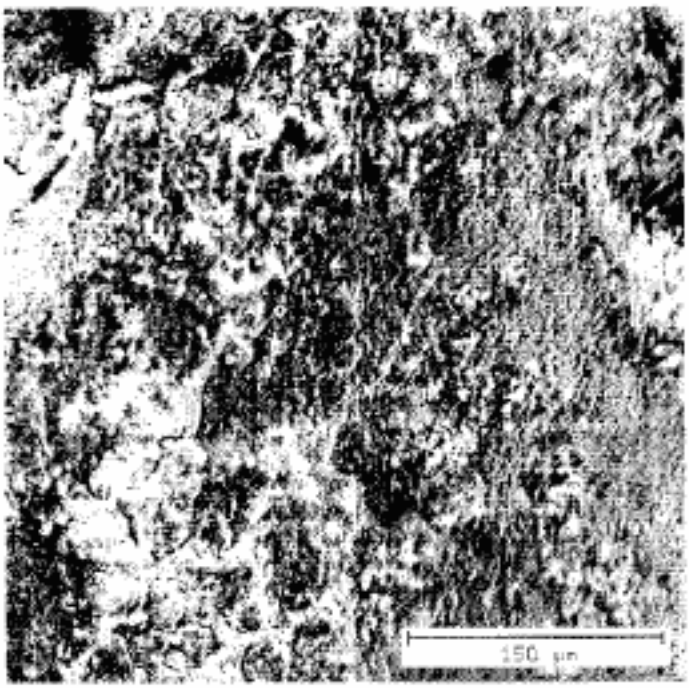

Bild 8 REM-Aufnahme der Bruchfläche mit dicker Schicht der Korrosionsprodukte, Probe 1.3/00/3664 V021

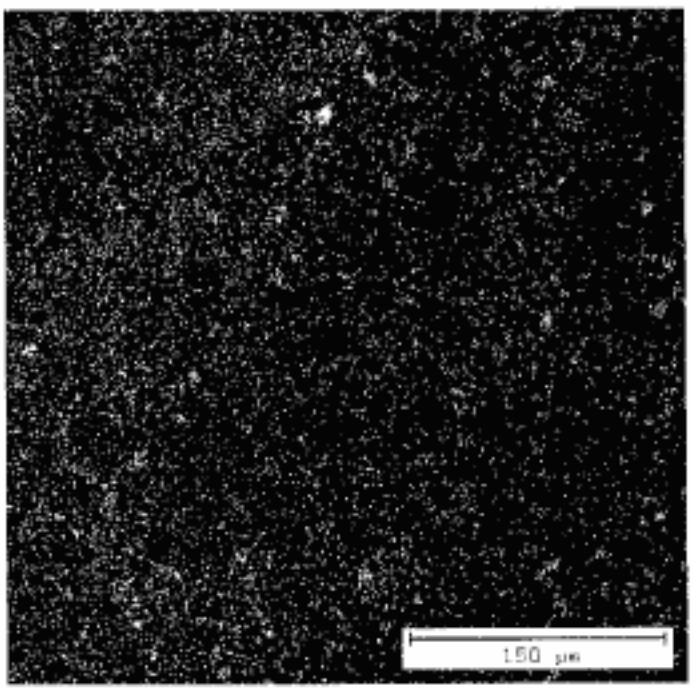

Bild 9 Siliziumverteilung im Bild 8

Bild 10 REM-Aufnahme der Bruchfläche mit dicker Schicht der Korrosionsprodukte, Probe 1.3/00/3664 V011

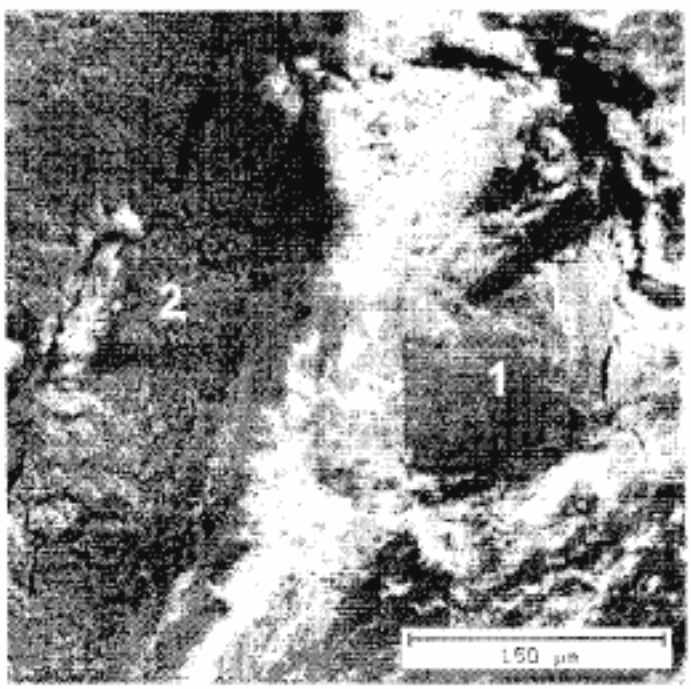

Bild 11 REM-Aufnahme der Bruchfläche, Probe 1.3/00/3664 V021

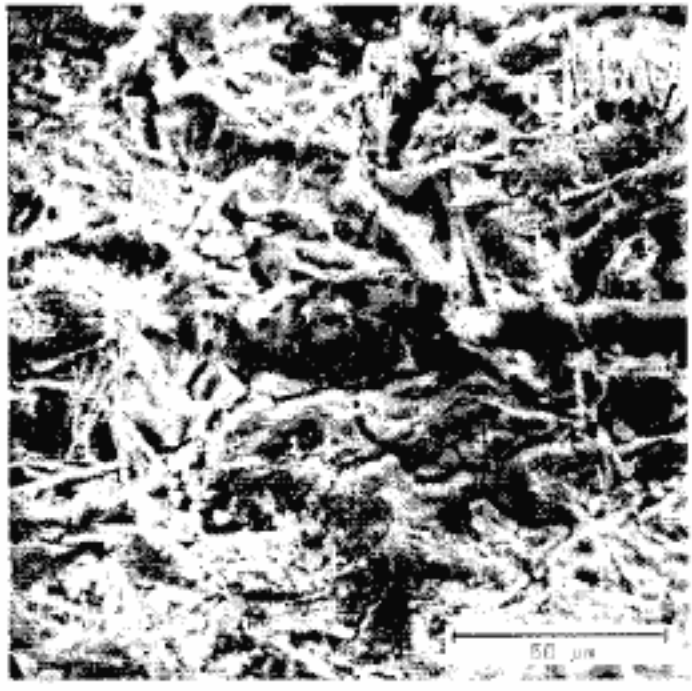

Bild 12 REM-Aufnahme eines Bruchflächenbereichs mit partiell abgeplatzter Schicht der Korrosionsprodukte, Probe 1.3/00/3664 V011

Bild 13 REM-Aufnahme eines Bruchflächenbereichs mit vollständig abgeplatzter Schicht der Korrosionsprodukte, Probe 1.3/00/3664 V011

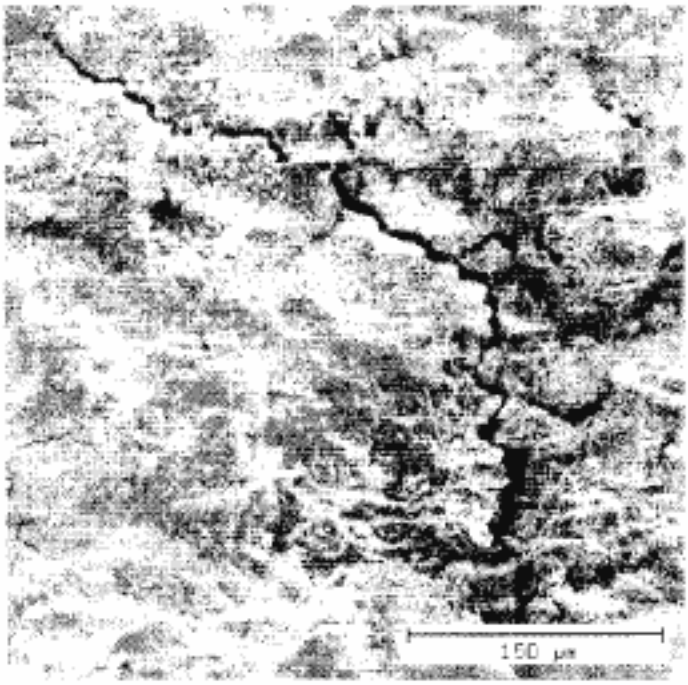

Bild 14 REM-Aufnahme eines Bruchflächenbereichs nach mechanischer Entfernung der Schicht der Korrosionsprodukte, Probe 1.3/00/3664 V011

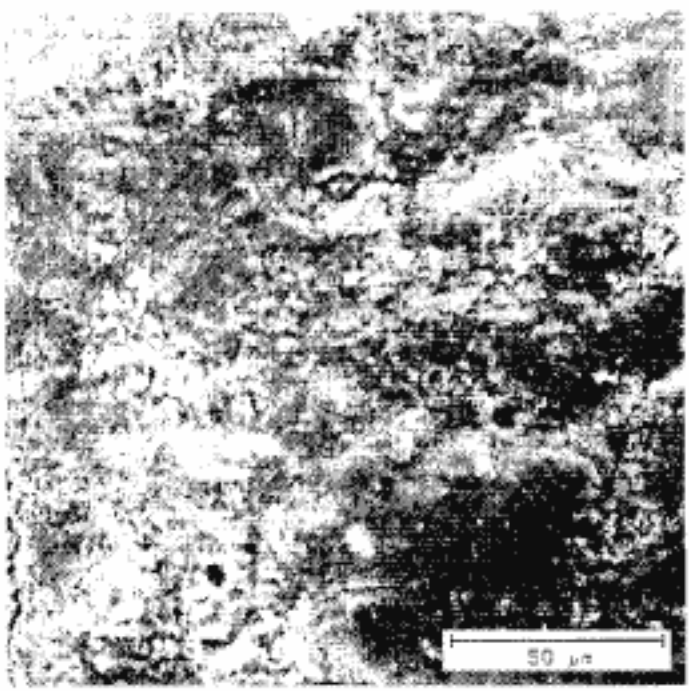

Bild 15 REM-Aufnahme eines Oberflächenbereichs nahe dem Bruch mit dicker Schicht der Korrosionsprodukte, Probe 1.3/00/3664 V021

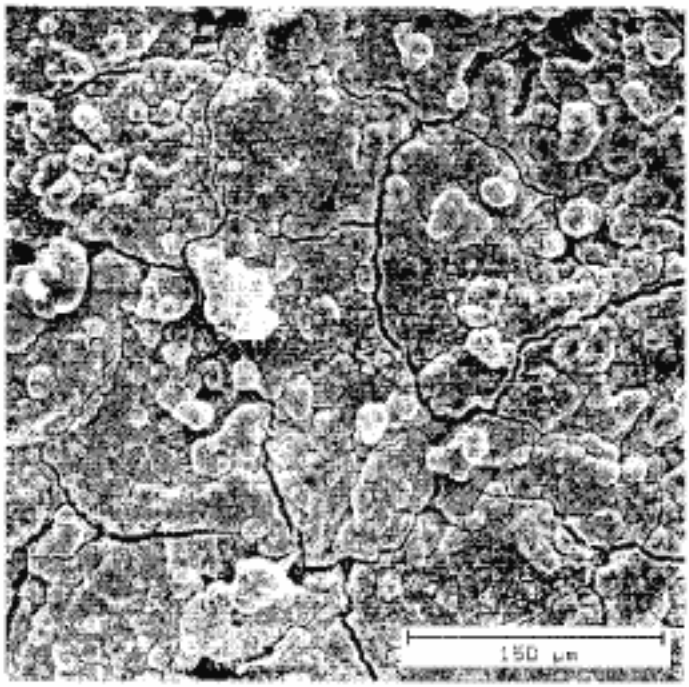

Bild 16 REM-Aufnahme eines Oberflächenbereichs nahe dem Bruch mit partiell abgeplatzter Schicht der Korrosionsprodukte, Probe 1.3/00/3664 V021

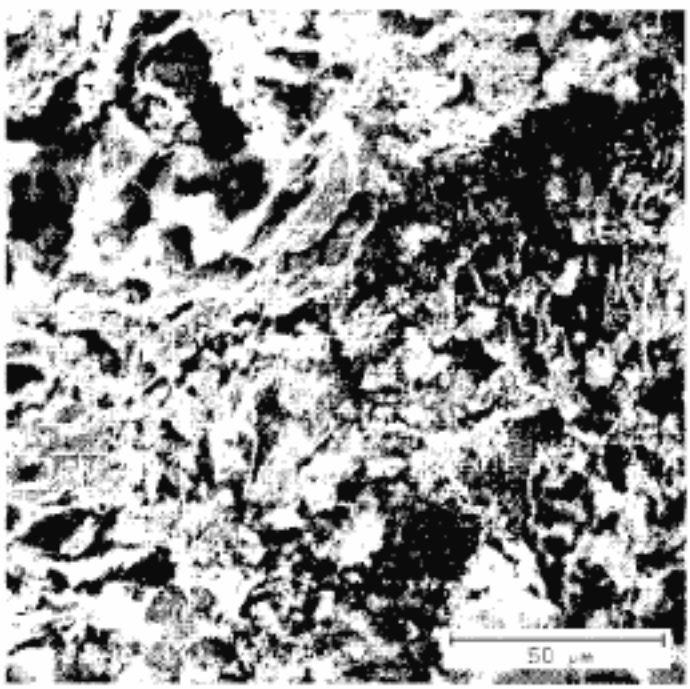

Bild 17 REM-Aufnahme eines Oberflächenbereichs nahe dem Bruch mit vollständig abgeplatzter Schicht der Korrosionsprodukte, Probe 1.3/00/3664 V021

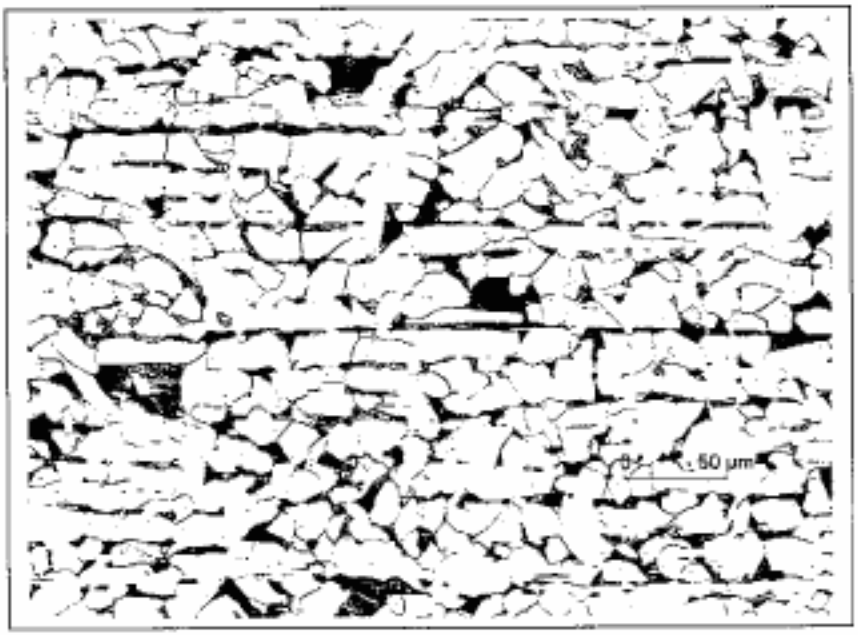

Bild 18 Probe 1.3/00/3664 G01 1

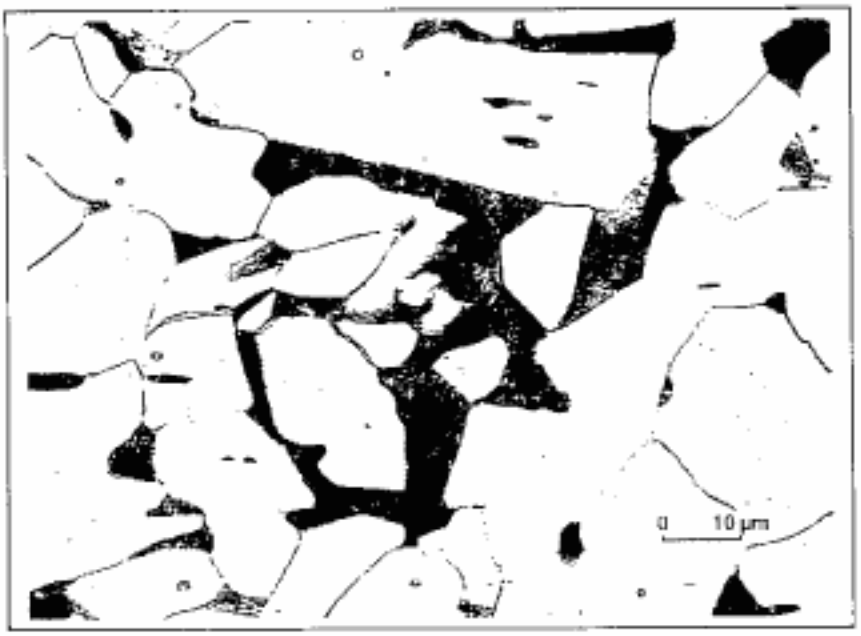

Bild 19 Probe 1.3/00/3664 G01 1

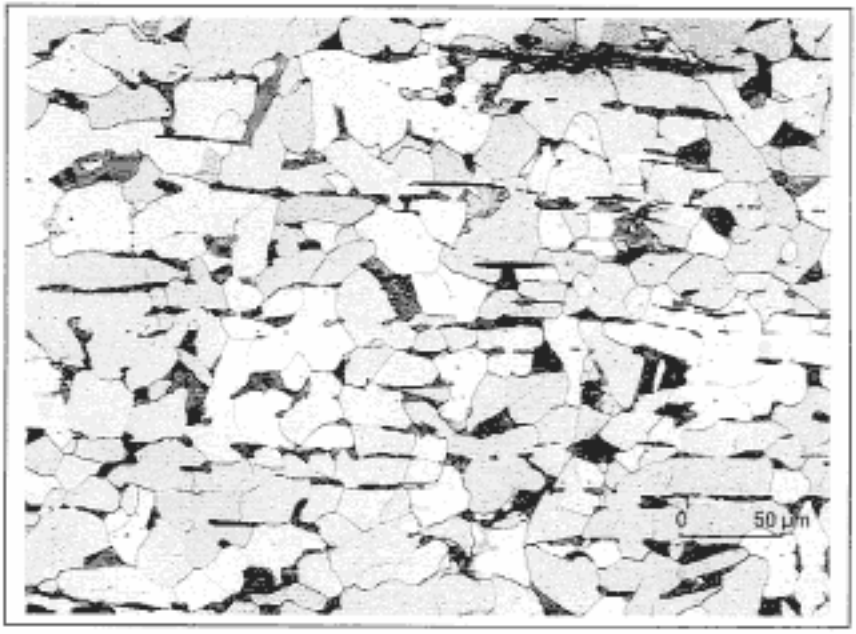

Bild 20 Probe 1.3/00/3664 G01 2

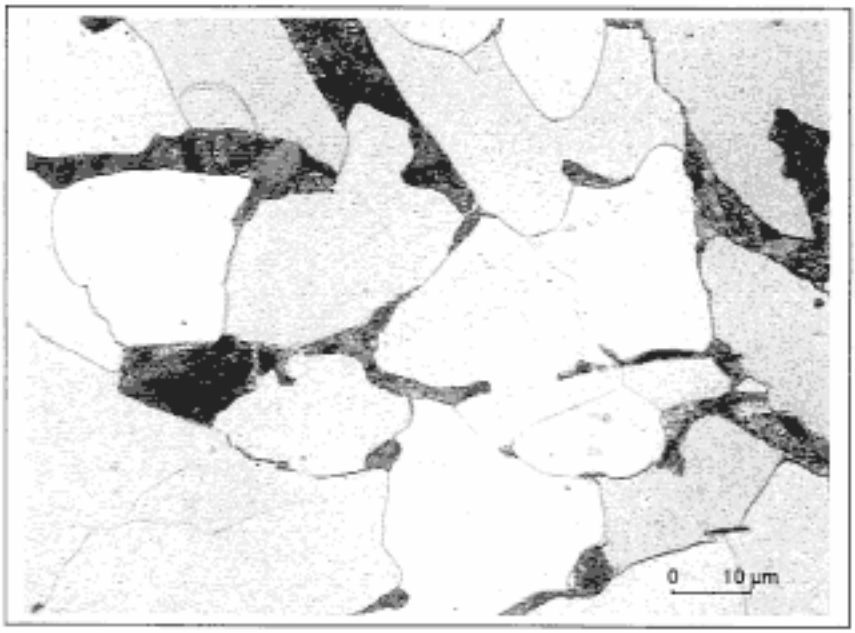

Bild 21 Probe 1.3/00/3664 G01 2

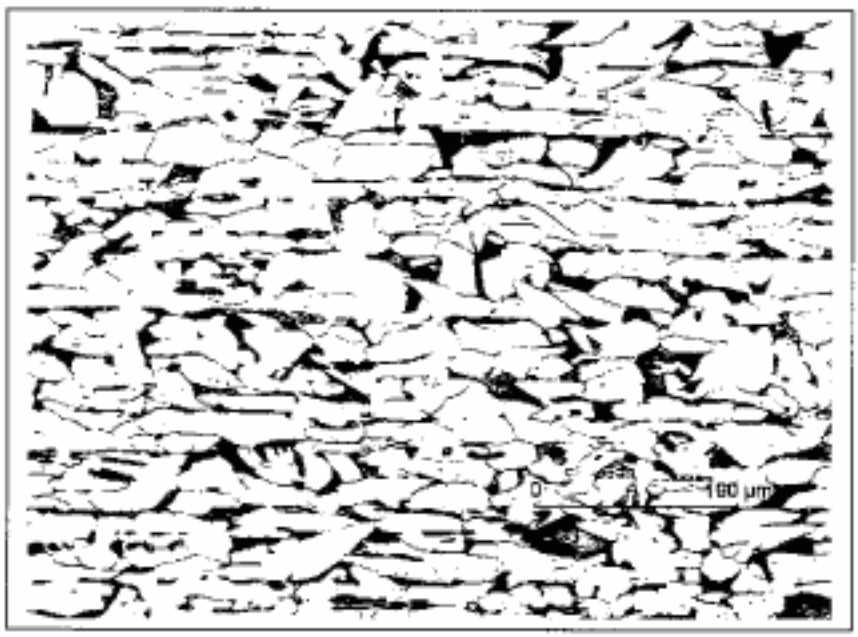

Bild 22 Probe 1.3/00/3664 G02 1

Bild 23 Probe 1.3/00/3664 G02 1

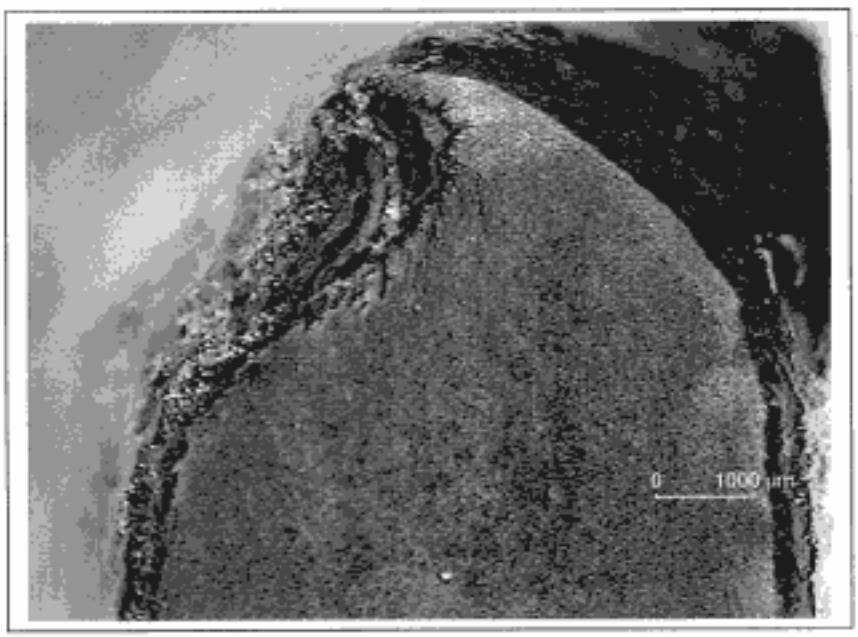

Bild 24 Probe 1.3/00/3664 G02 2

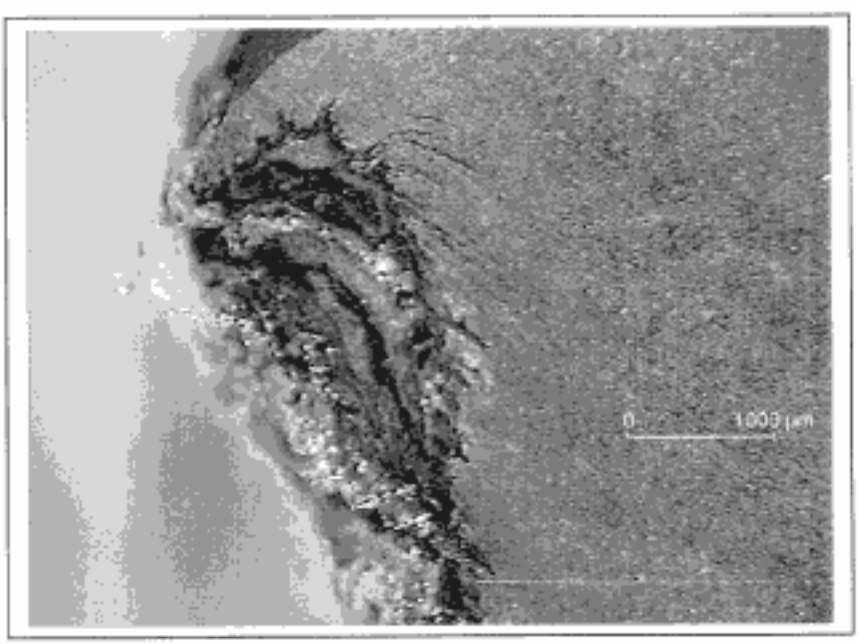

Bild 25 Probe 1.3/00/3664 G02 2

Bild 26 Probe 1.3/00/3664 G02 2

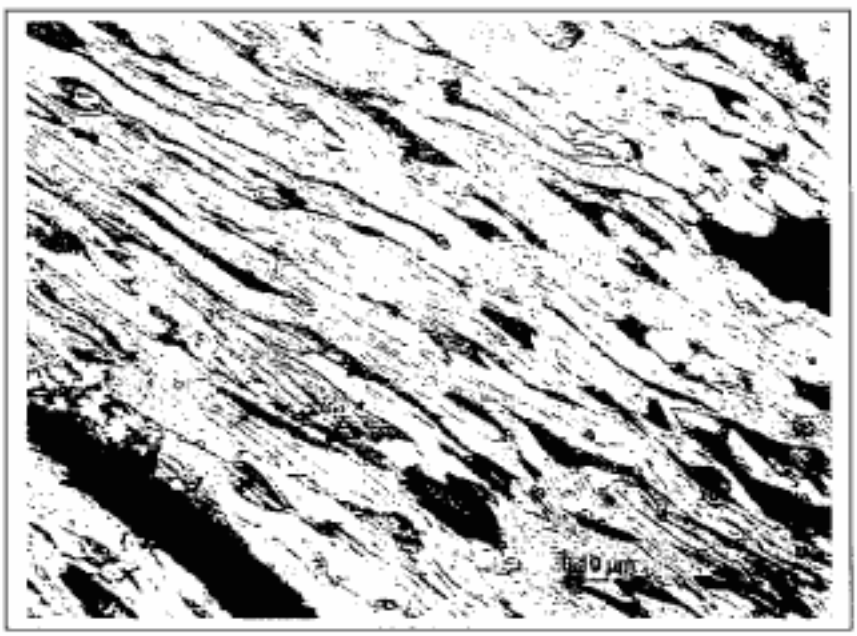

Bild 27 Probe 1.3/00/3664 G02 2

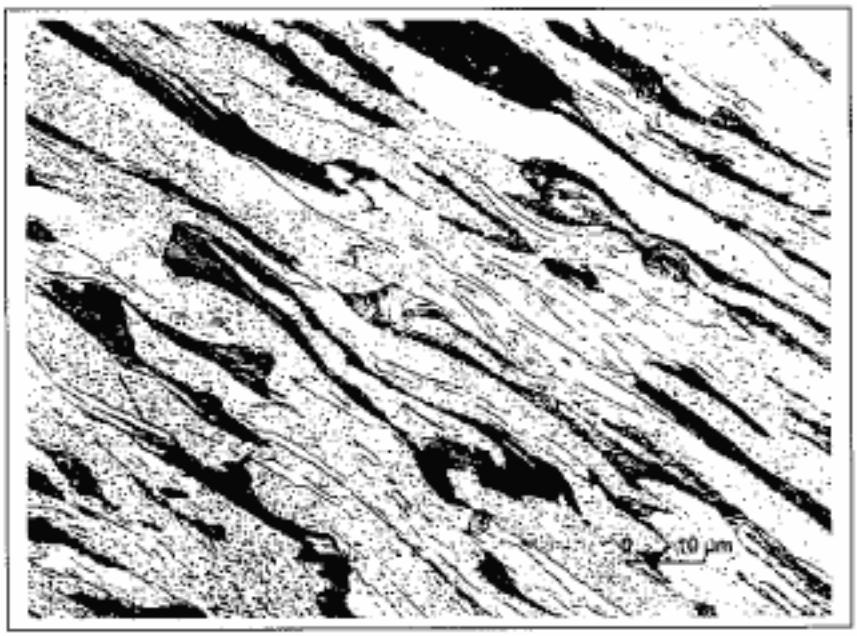

Bild 28 Probe 1.3/00/3664 G02 2

Bild 29 Probe 1.3/00/3664 G02 2

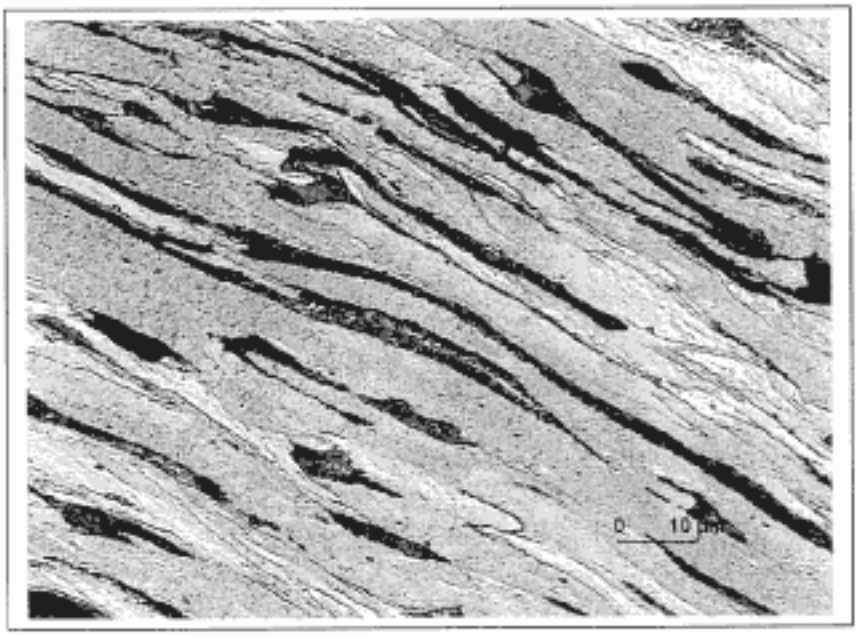

Bild 30 Probe 1.3/00/3664 G02 2

Bild 31 Probe 1.3/00/3664 G02 2

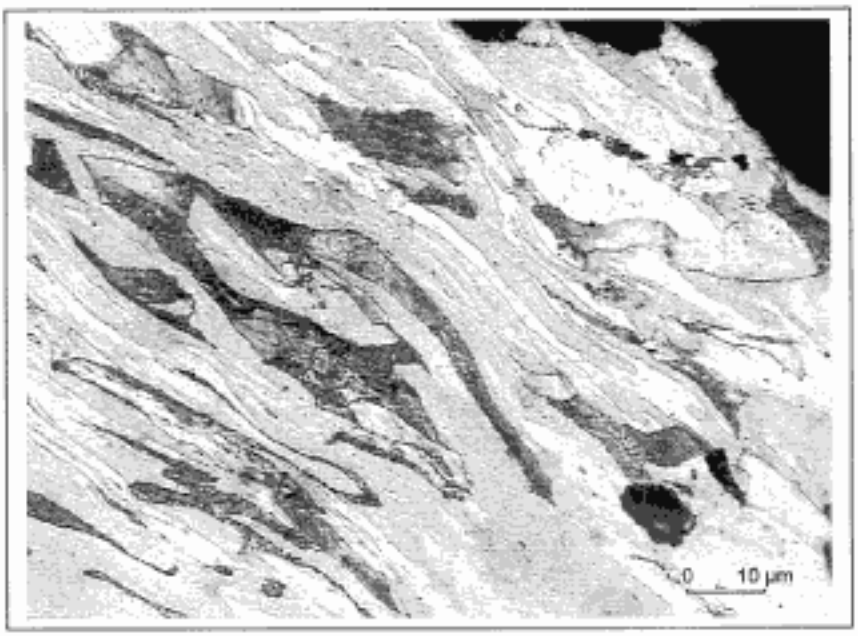

Bild 32 Probe 1.3/00/3664 G02 2

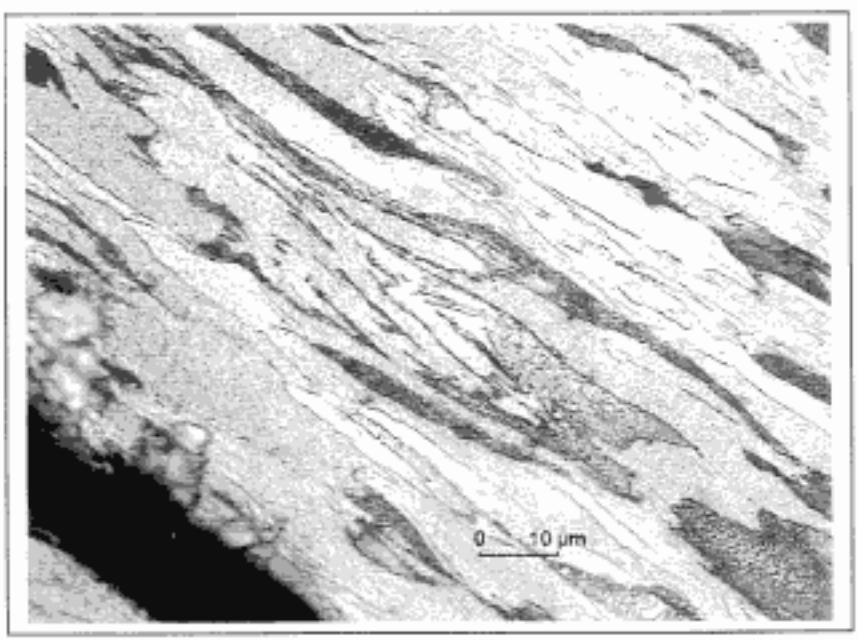

Bild 33 Probe 1.3/00/3664 G02 2

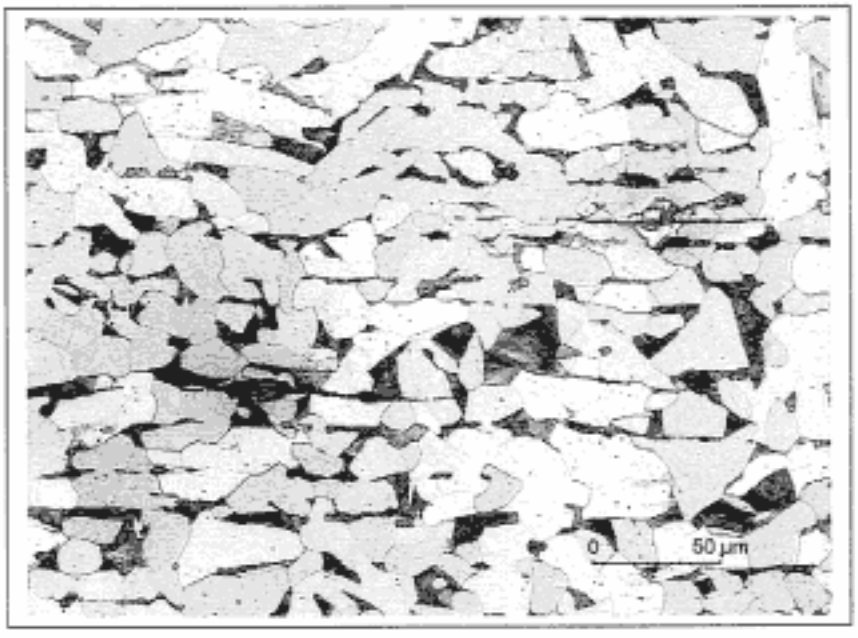

Bild 34 Probe 1.3/00/3664 G03 1

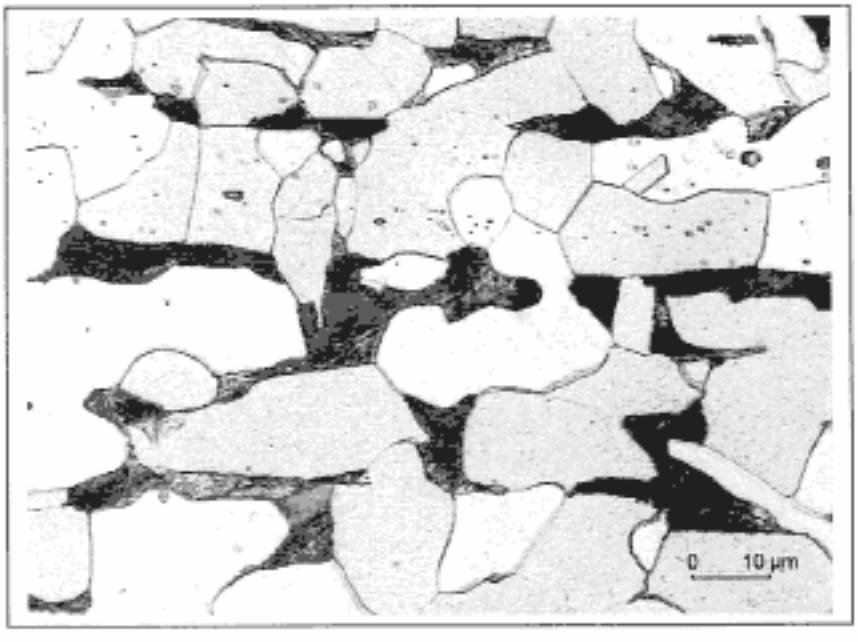

Bild 35 Probe 1.3/00/3664 G03 1

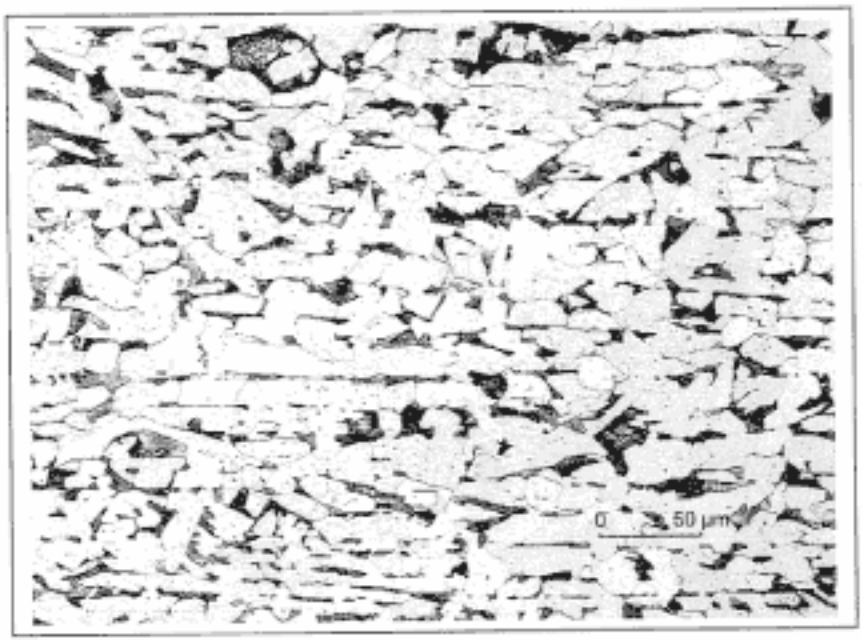

Bild 36 Probe 1.3/00/3664 G03 2

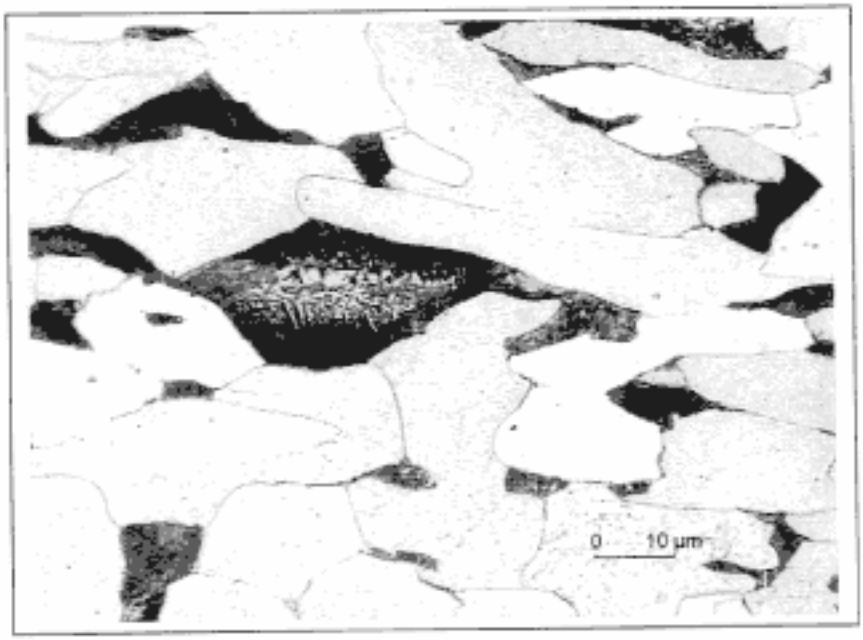

Bild 37 Probe 1.3/00/3664 G03 2

Materialprüfungsamt
des Landes Brandenburg

Stückanalyse

Prüfeinrichtung : GDS 750

Auftrag Nr.:1.3/00/3664

Auftraggeber : TOP STORY Filmproduktion GmbH

Dez.1.3/ Bearbeiter: Dipl.- Ing.(FH) H. Mettel

Datum :26.09.2000

Proben Nr:	Elementgehalt in Masse-% C	Si	Mn	P	S						N					
3664 S011	**0,19**	**0,189**	**0,54**	**0,005**	**0,014**							**0,005**					
Stabw.	0,006	0,001	0,002	0,000	0,001							0,000					

Mittelwert aus mindestens drei Messungen gebildet,
Stabw.= Standardabweichung

Aufgeführt werden, außer den ersten fünf Elementen, die zum Vergleich mit dem Regelwerk notwendigen Elemente, sowie Elemente mit Gehalten über 0,20%.

im Vergleich dazu:

St 37- 2 **Werkstoffnummer 1.0037** **EN 10025**

minimal:	0,00		0,00	0,000	0,000							0,000					
maximal:	0,21		1,50	0,050	0,050							0,011					
Bemerkung:	1)											2)					

1) Für Dicken gleich kleiner 16 mm - C gleich kleiner 0,20%
2) Je nach P- Gehalt N gleich kleiner 0,012%

Tabelle 4: Stückanalyse mittels Glimmentladungsspektrometrie sowie (falls angegeben) Vergleichswerte aus dem Regelwerk

Materialprüfungsamt
des Landes Brandenburg

Vickershärteprüfung
nach EN ISO 6507-1

Auftraggeber :	TOP STORY Filmproduktion GmbH
Auftrag :	1.3/00/3664
Datum :	27.09.2000

Prüfer:	Dipl. Ing. (FH) H. Mettel
Prüfmaschine:	Shimadzu HMV-2000
Prüfbereich:	HV 0,05
Werkstoff:	Stahl

Probe / Schliff
3664 G012

Mittelwert	Min.	Max.	S-abw.
306	281	341	24

Nr.	x[mm]	y[mm]	d1[µm]	d2[µm]	HV
1	0,50	0,00	16,8	16,4	338
2	1,00	0,00	15,9	17,0	341
3	1,50	0,00	16,8	17,7	312
4	2,00	0,00	17,6	18,2	289
5	2,50	0,00	18,0	17,5	294
6	3,00	0,00	17,8	18,2	286
7	3,50	0,00	18,0	18,4	281
8	4,00	0,00	16,9	18,7	291
9	4,50	0,00	18,1	17,5	291
10	5,00	0,00	15,8	17,4	338

Tabelle 5: Mikrohärteprüfung

Materialprüfungsamt
des Landes Brandenburg

Vickershärteprüfung
nach EN ISO 6507-1

Auftraggeber :	TOP STORY Filmproduktion GmbH
Auftrag :	1.3/00/3664
Datum :	28.09.2000

Prüfer:	Dipl. Ing. (FH) H. Mettel
Prüfmaschine:	Shimadzu HMV-2000
Prüfbereich:	HV 0,05
Werkstoff:	Stahl

Probe / Schliff
3664 G022

Mittelwert	Min.	Max.	S-abw.
457	360	619	62

Nr.	x[mm]	y[mm]	d1[µm]	d2[µm]	HV
1	0,00	0,00	13,2	13,6	515
2	0,50	0,00	13,1	14,1	502
3	1,00	0,00	14,2	14,0	466
4	1,50	0,00	12,9	14,0	515
5	2,00	0,00	14,6	15,3	415
6	2,50	0,00	14,4	15,0	429
7	3,00	0,00	14,2	14,5	450
8	3,50	0,00	14,9	14,3	434
9	4,00	0,00	15,3	15,8	384
10	4,50	0,00	14,7	15,0	419
11	5,00	0,00	10,7	13,8	619
12	5,50	0,00	13,9	14,6	455
13	6,00	0,00	14,4	15,7	410
14	6,50	0,00	14,1	14,3	461
15	7,00	0,00	13,9	14,1	472
16	7,50	0,00	15,1	17,0	360

Tabelle 6: Mikrohärteprüfung

Materialprüfungsamt
des Landes Brandenburg

Vickershärteprüfung
nach EN ISO 6507-1

Auftraggeber :	TOP STORY Filmproduktion GmbH
Auftrag :	1.3/00/3664
Datum :	28.09.2000

Prüfer:	Dipl. Ing. (FH) H. Mettel
Prüfmaschine:	Shimadzu HMV-2000
Prüfbereich:	HV 0,05
Werkstoff:	Stahl

Probe / Schliff
3664 G032

Mittelwert	Min.	Max.	S-abw.
371	225	439	54

Nr.	x[mm]	y[mm]	d1[µm]	d2[µm]	HV
1	0,00	0,00	18,6	16	309
2	0,50	0,00	15,4	13,8	434
3	1,00	0,00	19,5	21,1	225
4	1,50	0,00	15,6	14,8	401
5	2,00	0,00	14,4	14,6	439
6	2,50	0,00	14,7	16,2	388
7	3,00	0,00	15,9	15,7	371
8	3,50	0,00	15,8	14,6	401
9	4,00	0,00	15,4	15,8	379
10	4,50	0,00	14,4	15,0	429
11	5,00	0,00	16,9	16,9	324
12	5,50	0,00	15,8	15,8	371
13	6,00	0,00	15,3	15,7	388
14	6,50	0,00	15,6	15,7	379
15	7,00	0,00	16,6	16,9	331
16	7,50	0,00	15,8	16,4	360

Tabelle 7: Mikrohärteprüfung